Developmental Biology 369 (2012) 211–222

Contents lists available at SciVerse ScienceDirect

Developmental Biology

journal homepage: www.elsevier.com/locate/developmentalbiology

The mouse Wnt/PCP protein Vangl2 is necessary for migration of facial branchiomotor neurons, and functions independently of Dishevelled

Derrick M. Glasco [a,1], Vinoth Sittaramane [a], Whitney Bryant [a], Bernd Fritzsch [b], Anagha Sawant [a], Anju Paudyal [c,d], Michelle Stewart [c], Philipp Andre [e], Gonçalo Cadete Vilhais-Neto [f], Yingzi Yang [e], Mi-Ryoung Song [g], Jennifer N. Murdoch [c,d], Anand Chandrasekhar [a,*]

[a] Division of Biological Sciences, Room 340D Bond Life Sciences Center, University of Missouri, 1201 Rollins Street, Columbia, MO 65211, USA
[b] Department of Biological Sciences, University of Iowa, Iowa City, IA 52242, USA
[c] Developmental Genetics Section, Medical Research Council Harwell, Oxfordshire, OX11 ORD, UK
[d] Centre for Biomedical Sciences, School of Biological Sciences, Royal Holloway University of London, Egham, TW20 0EX, UK
[e] Developmental Genetics Section, National Human Genome Research Institute, NIH, Bethesda, MD 20892, USA
[f] IGBMC, UMR 7104, Inserm U964, Université de Strasbourg, Illkirch, F-67400, France
[g] Bioimaging and Cell Dynamics Research Center, School of Life Sciences, Gwangju Institute of Science and Technology, Gwangju 500-712, South Korea.

ARTICLE INFO

Article history:
Received 24 April 2012
Received in revised form
19 June 2012
Accepted 27 June 2012
Available online 4 July 2012

Keywords:
Facial branchiomotor neuron migration
Planar Cell Polarity signaling
Van Gogh-like 2
Disheveled
Protein tyrosine kinase 7
Looptail

ABSTRACT

During development, facial branchiomotor (FBM) neurons, which innervate muscles in the vertebrate head, migrate caudally and radially within the brainstem to form a motor nucleus at the pial surface. Several components of the Wnt/planar cell polarity (PCP) pathway, including the transmembrane protein Vangl2, regulate caudal migration of FBM neurons in zebrafish, but their roles in neuronal migration in mouse have not been investigated in detail. Therefore, we analyzed FBM neuron migration in mouse *looptail* (*Lp*) mutants, in which *Vangl2* is inactivated. In *Vangl2*$^{Lp/+}$ and *Vangl2* $^{Lp/Lp}$ embryos, FBM neurons failed to migrate caudally from rhombomere (r) 4 into r6. Although caudal migration was largely blocked, many FBM neurons underwent normal radial migration to the pial surface of the neural tube. In addition, hindbrain patterning and FBM progenitor specification were intact, and FBM neurons did not transfate into other non-migratory neuron types, indicating a specific effect on caudal migration.

Since loss-of-function in some zebrafish Wnt/PCP genes does not affect caudal migration of FBM neurons, we tested whether this was also the case in mouse. Embryos null for *Ptk7*, a regulator of PCP signaling, had severe defects in caudal migration of FBM neurons. However, FBM neurons migrated normally in *Dishevelled* (*Dvl*) *1/2* double mutants, and in zebrafish embryos with disrupted *Dvl* signaling, suggesting that *Dvl* function is essentially dispensable for FBM neuron caudal migration. Consistent with this, loss of *Dvl2* function in *Vangl2*$^{Lp/+}$ embryos did not exacerbate the *Vangl2*$^{Lp/+}$ neuronal migration phenotype. These data indicate that caudal migration of FBM neurons is regulated by multiple components of the Wnt/PCP pathway, but, importantly, may not require Dishevelled function. Interestingly, genetic-interaction experiments suggest that rostral FBM neuron migration, which is normally suppressed, depends upon *Dvl* function.

Introduction

Neuronal migration is an essential aspect of nervous system development, and contributes to the formation of functional neural networks and distinct neural layers in the mammalian brain. Radial migration, which accompanies the maturation of all neurons in the central nervous system, involves cell body translocation from the ventricular proliferative zone towards the outer (pial) surface of the brain, often along radial glial fibers. Several types of neurons also undergo tangential migration, which is glia-independent and orthogonal to the direction of radial migration (Hatten, 2002; Marin and Rubenstein, 2003; Nadarajah and Parnavelas, 2002).

In the embryonic hindbrain, facial branchiomotor (FBM) neurons undergo both radial and tangential migration, and thus make an excellent model system for studying neuronal migration mechanisms. In mice, FBM neurons are born in rhombomere 4 (r4) and by E10.5 begin to migrate caudally (tangentially) into r6,

* Corresponding author. Fax: +1 573 884 9676.
E-mail address: AnandC@missouri.edu (A. Chandrasekhar).
[1] Present address: Department of Biology, Bob Jones University, Greenville, SC 29614, USA.

0012-1606/$ - see front matter © 2012 Elsevier Inc. All rights reserved.
http://dx.doi.org/10.1016/j.ydbio.2012.06.021

fully forming the facial motor nucleus near the pial surface of r6 by E14.5 (Carpenter et al., 1993; Fritzsch et al., 1993; Garel et al., 2000). Diverse classes of molecules, including members of the non-canonical Wnt/planar cell polarity (PCP) pathway, regulate FBM neuron migration in both zebrafish and mice (Song, 2007). In *Xenopus* and zebrafish, Wnt/PCP signaling components are required for proper convergence and extension cell movements during gastrulation (Darken et al., 2002; Park and Moon, 2002; Tada et al., 2002; Wallingford and Harland, 2002). In mice, Wnt/PCP proteins are additionally implicated in hair follicle orientation, stereocilia orientation in the inner ear, and neural tube closure (Curtin et al., 2003; Devenport and Fuchs, 2008; Doudney and Stanier, 2005; Goodrich, 2008; Kallay et al., 2006; Montcouquiol et al., 2003; Ravni et al., 2009; Torban et al., 2004a, 2004b; Ybot-Gonzalez et al., 2007).

Given their roles in mediating directed cell migrations and cell polarity events in developing tissues, it is not surprising that Wnt/PCP genes also play critical roles in FBM neuron migration. However, it is not clear whether FBM neuron migration is truly a PCP process. In zebrafish, FBM neurons migrate normally in several Wnt/PCP mutants, defective for *wnt5b*, *wnt11*, and *glypican4/6*, which exhibit strong convergence and extension movement (PCP) defects (Bingham et al., 2002; Jessen et al., 2002) (Fig. 8). Conversely, FBM neurons fail to migrate caudally in other Wnt/PCP mutants, defective for *fzd3a*, *celsr2*, *pk1b*, and *scrib*, which exhibit no convergence and extension defects (Wada et al., 2005, 2006; Mapp et al., 2011) (Fig. 8). These observations suggest that FBM neuron migration and a PCP process like convergence and extension movements are regulated independently in zebrafish. Due to the importance of these cellular movements for nervous system development, we wondered whether these processes were also regulated independently in mammals. Therefore, we examined FBM neuron migration in mouse mutants *looptail* and *chuzhoi*, which inactivate Van gogh-like 2 (Vangl2) and Protein tyrosine kinase 7 (Ptk7), respectively, and exhibit strong defects in several PCP processes (Kibar et al., 2001; Lu et al., 2004; Montcouquiol et al., 2006; Murdoch et al., 2001; Paudyal et al., 2010).

Consistent with observations that FBM neuron migration and PCP processes may be regulated independently, it appears that Wnt/PCP signaling may itself play only a minor role in FBM neuron migration. First, although Wnt5a- and Wnt7a-coated beads can attract FBM neurons in hindbrain explants, these neurons still migrate caudally in *Wnt5a* and *Wnt7a* mutant embryos (Vivancos et al., 2009), suggesting a redundant or minor role for Wnts in this process, as shown previously with zebrafish *wnt5b* and *wnt11* mutants (Jessen et al., 2002). Second, abrogation of PCP-specific Dishevelled (Dvl) function in zebrafish using a dominant negative approach had no effect on FBM neuron migration (Jessen et al., 2002), suggesting that Dvl function may be dispensable for caudal migration. We have tested this hypothesis by extending the Dvl dominant-negative analysis in zebrafish, and by examining FBM neuron migration in *Dvl* knockout mice.

Vivancos et al. (2009) found that FBM neurons failed to migrate caudally in *Vangl2* mutant mice harboring the *looptail* (*Lp*) S464N mutation (Murdoch et al., 2001). We report here that in a different *Lp* mutant (D255E; Kibar et al., 2001), and also in *Vangl2* knockout mice (Song et al., 2010), caudal migration of FBM neurons was abolished. FBM neurons also failed to migrate in *Ptk7* mutant embryos. Importantly, FBM neurons migrated normally in *Dvl1/2* double mutants, and in zebrafish embryos with disrupted *dvl* signaling. Our data demonstrate that FBM neuron migration and PCP processes are regulated independently in mouse, as in zebrafish, and that *Dvl* function is largely dispensable for caudal FBM neuron migration (Fig. 8). Interestingly, genetic-interaction experiments suggest that rostral FBM neuron migration, which is normally suppressed, depends upon *Dvl* function.

Materials and methods

Animals

Mouse colonies were maintained and embryos collected according to the requirements of the Animals (Scientific Procedures) Act 1986 of the UK Government, and various institutional guidelines, including those of the University of Missouri Animal Care and Use Committee (ACUC). Zebrafish colonies were maintained and embryos collected following standard protocols approved by the University of Missouri ACUC.

Mouse lines and genotyping

The *Vangl2*$^{Lp\text{-}m1Jus}$, *Vangl2*^{del}, *Celsr1*^{Crsh}, *Dvl1*^{tm1Awb}, *Dvl2*^{tm1Awb}, *Ptk7*^{chuzhoi}, and *SE1::gfp* mouse lines have been described previously (Curtin et al., 2003; Hamblet et al., 2002; Kibar et al., 2001; Lijam et al., 1997; Shirasaki et al., 2006; Song et al., 2010). The *Dvl1* and *Dvl2* lines were purchased from Jackson Labs. Genotyping of the *Vangl2*$^{Lp\text{-}m1Jus}$ allele (referred to as *Vangl2*^{Lp}, from here on) was performed using primers 5′-GGTTCAG-TTTGCCGTTTCTC-3′ and 5′-CCCTCCTTCCCCTAAACCTT-3′, followed by sequencing of the PCR product to identify the T1228A mutation. Genotyping of *Celsr1*^{Crsh} was performed similarly using primers 5′- AATTCAGGTGAGTGTGTTGGA-3′ and 5′-GTCACCACT-CAGTAGGTCCAG-3′ to identify the A3119G mutation.

For timed matings, noon on the day of a copulation plug was defined as embryonic day (E)0.5. Embryos were staged using standard morphological criteria (Nagy, 2003) before fixation.

Zebrafish

Maintenance of zebrafish stocks, and collection and development of embryos in embryo medium were carried out as described previously (Bingham et al., 2002; Westerfield, 1995). To facilitate analysis of branchiomotor neuron development, *Tg*(*isl1*:*gfp*) fish (Higashijima et al., 2000) were used for all experiments.

RNA injection

The expression constructs encoding different Dishevelled (Dvl) and Daam1 proteins in pCS2 were obtained from indicated sources by Drs. Oni Mapp and Victoria Prince (University of Chicago) and kindly provided to us: *Xenopus* Dvl full-length, and Dvl deltaC (Tada and Smith, 2000); Dvl delta PDZ (Xdd1), Dvl delta N, and human N-Daam1 (Habas et al., 2001). RNAs were prepared and injected as described previously (Sittaramane et al., 2009). Embryos at the 1–4 cell stage were injected with RNA (200 pg/embryo) and examined at 24–48 hours post fertilization (hpf) for FBM neuron migration phenotypes. To monitor the amounts of protein produced from the various RNAs, ~50 embryos per treatment were collected at 20 hpf, when FBM neurons are migrating, solubilized in lysis buffer, and processed for Western blot analysis with anti-myc (all Dvl constructs) and anti-FLAG (N-Daam1) antibodies (anti-myc: Cell Signaling Technologies; anti-FLAG: Sigma–Aldrich) (Fig. S6).

In situ hybridization

Hindbrains were processed for in situ hybridization as described previously (Qu et al., 2010). For imaging, hindbrains were either mounted in open book preparations or embedded in OCT (Ted Pella) for cryostat sectioning. Riboprobes used in this study were *Dvl3* (Tissir and Goffinet, 2006), *Gata3* (Karis et al., 2001), *Hb9* (Qu et al., 2010), *Mash1* and *Math3* (Tiveron et al.,

2003), *Pk1* (Song et al., 2006), *Tbx20* (Kraus et al., 2001), *Vangl2* (Tissir and Goffinet, 2006), and *Wnt5a* (Song et al., 2006).

Immunohistochemistry

For NF160 neurofilament staining, mouse embryos were processed as previously described (Qu et al., 2010). Embryos were stored in 75% glycerol and imaged on an Olympus SZX12 stereomicroscope. Whole-mount immunohistochemistry of zebrafish embryos (zn5, GFP, myc antibodies) was performed and imaged as described previously (Sittaramane et al., 2009).

Demarcation of rhombomere boundaries

Rhombomere boundaries in the mouse wild-type hindbrain were defined using several criteria: In E12.5 embryos processed for *Tbx20* in situ, the caudal limit of the trigeminal (nV) motor neurons was defined as the r2/3 boundary, the rostral edge of the FBM neuron expression domain was defined as the r3/4 boundary, and the sharp indentation in the lateral edge of the migrating column was defined as the r4/5 boundary (Fig. 2D). For E14.5 embryos, the approximate locations of r2, r5 and r6 were defined by the positions of the nV (r2) and FBM (r5, r6) neurons, respectively (Fig. 2G). For E12.5 embryos expressing GFP in cranial motor neurons, the r3/4 and r4/5 boundaries were defined as for *Tbx20* in situ. These boundaries also coincided with the fan-shaped genu of FBM axons extending laterally toward their exit points (Fig. 2A), and with the location of the abducens motor nucleus (nVI) in r6 (Fig. 2B).

Rhombomere boundaries in mouse mutant hindbrains were assumed to be coincident with those in wild-type embryos because the identities and sizes of rhombomere compartments (r3–r5) were not affected in *Vangl2*$^{Lp/+}$, *Vangl2*$^{Lp/Lp}$, *Celsr1*$^{Crsh/+}$ and *Celsr1*$^{Crsh/Crsh}$ embryos (Qu et al., 2010; Thoby-Brisson et al., 2012). One exception was *Dvl1/2* double mutant embryos where r3 appeared to be longer at the expense of r4 (Fig. 6D) with no appreciable change relative to wild-type in the overall length of the hindbrain region spanning r2–r6.

Rhombomere boundaries in zebrafish were established based on the characteristic patterns of zn5+ve commissural axon fascicles (Bingham et al., 2002).

Results

FBM neurons fail to migrate caudally in Vangl2 mutants

In mouse, facial branchiomotor (FBM) neurons start differentiating in rhombomere (r) 4 at E10.5, as shown by expression of *Tbx20*, a marker for branchiomotor and visceromotor neurons (Coppola et al., 2005), (Fig. 1A; Song et al., 2006), and start migrating caudally shortly thereafter. By E12, there is a continuous stream of FBM neurons migrating caudally out of r4 into r5 and r6, where they undergo radial migration toward the pial surface (Fig. 1B; Garel et al., 2000). Previous studies in zebrafish and mice have demonstrated roles for several Wnt/PCP genes in FBM neuron migration (Bingham et al., 2002; Carreira-Barbosa et al., 2003; Qu et al., 2010; Vivancos et al., 2009; Wada et al., 2006). The Wnt/PCP gene *Vangl2* is expressed in FBM neurons and in adjacent tissues during the migration period (Fig. 1C–F; six embryos per time point; compare Fig. 1F and Fig. S2A′ to visualize FBM neuron location in hindbrain cross section; see also Fig. 8 in Song et al., 2006). Therefore, we tested whether FBM neuron migration was affected in *looptail* (*Lp*) mutant embryos harboring a D255E mutation in the C-terminal cytoplasmic domain of Vangl2 (Torban et al., 2004b) that abolishes localization to the plasma membrane (Torban et al., 2007).

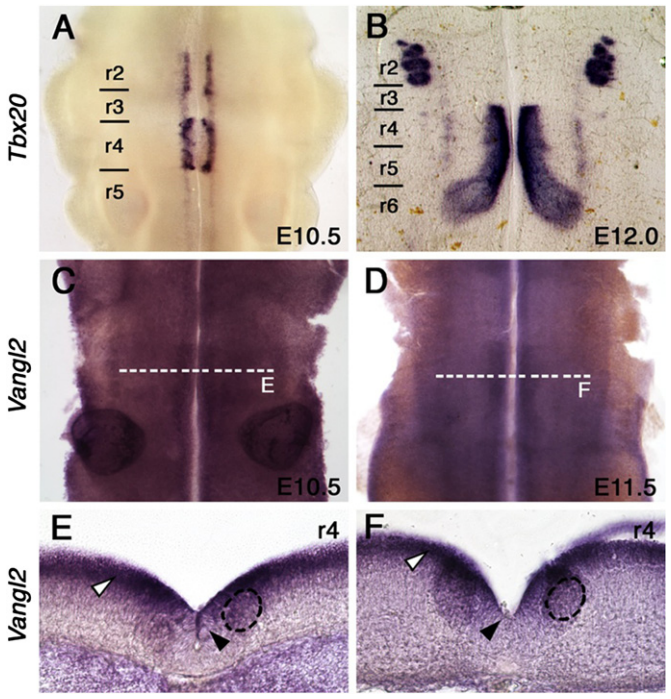

Fig. 1. *Vangl2* expression in the hindbrain. (A)–(D), ventricular views of flat-mounted hindbrains processed for in situ hybridization (ISH) with *Tbx20* (A, B) and *Vangl2* (C, D) probes. At E10.5 (A), *Tbx20* is expressed in trigeminal branchiomotor neurons in r2–r3 and facial branchiomotor (FBM) neurons in r4. By E12.0 (B), *Tbx20* expression is maintained in laterally-migrated trigeminal branchiomotor neurons in r2–r3 and caudally migrating FBM neurons spanning r4–r6. At the onset of FBM neuron migration, E10.5 (C) and E11.5 (D), *Vangl2* mRNA is expressed at all axial levels of the hindbrain. Stronger expression is seen near the midline corresponding to the location of the FBM neurons. (E) and (F), Coronal sections (r4 level) of embryos in (C) and (D). At E10.5 (E), *Vangl2* is expressed in the ventricular zone (white arrowhead) and in the FBM neuron domain (dotted circle), with low expression in the floorplate (black arrowhead). At E11.5 (F), *Vangl2* expression is maintained in the ventricular zone (white arrowhead) and in the FBM neuron domain (dotted circle), and reduced in floorplate cells (black arrowhead).

We first examined FBM neuron migration in the *SE1::gfp* background, in which all cranial motor neurons express GFP (Song et al., 2006). In WT embryos at E11.5 and E12.5, FBM neurons formed longitudinal streams of migrating cells spanning r4 to r6, then migrated dorso-laterally and radially within r6 (Fig. 2A and Fig. S1A; $n=10$ embryos). In contrast, FBM neurons largely failed to migrate caudally out of r4 in both *Vangl2*$^{Lp/+}$ and *Vangl2*$^{Lp/Lp}$ embryos (Fig. 2B, C; *Lp*/+ ($n=17$), *Lp*/*Lp* (8); Table S1), although some neurons migrated dorso-laterally, especially in the vicinity of the r4/r5 boundary (Fig. S1B, C). Interestingly, some GFP+ve cells were also found laterally in r3 in several *Vangl2*$^{Lp/+}$ and *Vangl2*$^{Lp/Lp}$ embryos, but never in WT embryos, suggestive of aberrant rostral migration (Fig. S1; *Lp*/+ (39/47), *Lp*/*Lp* (9/26); Table S1). *Tbx20* in situ revealed that by E12.5, WT FBM neurons migrated radially towards the pial surface within r6 to form the facial motor nucleus (nVII) (Fig. 2D and Fig. S2A–A″; $n=7$), which was fully formed by E14.5 (Fig. 2G; $n=3$). Interestingly, although FBM neurons in *Vangl2*$^{Lp/+}$ remained mostly confined to r4, they still underwent their dorso-lateral and radial migrations to form elongated nuclei at the pial surface, spanning r3 to r5 (Fig. 2E, H and Fig. S2B–B″; E12.5 ($n=8$), E14.5 (4)). In *Vangl2*$^{Lp/Lp}$ mutants, FBM neurons remained within r4 and most failed to migrate radially to the pial surface of the neural tube (Fig. 2F, I and Fig. S2C–C″; E12.5 ($n=3$), E14.5 (6); see also Vivancos et al., 2009). Since craniorachischisis (open neural tube) occurs in

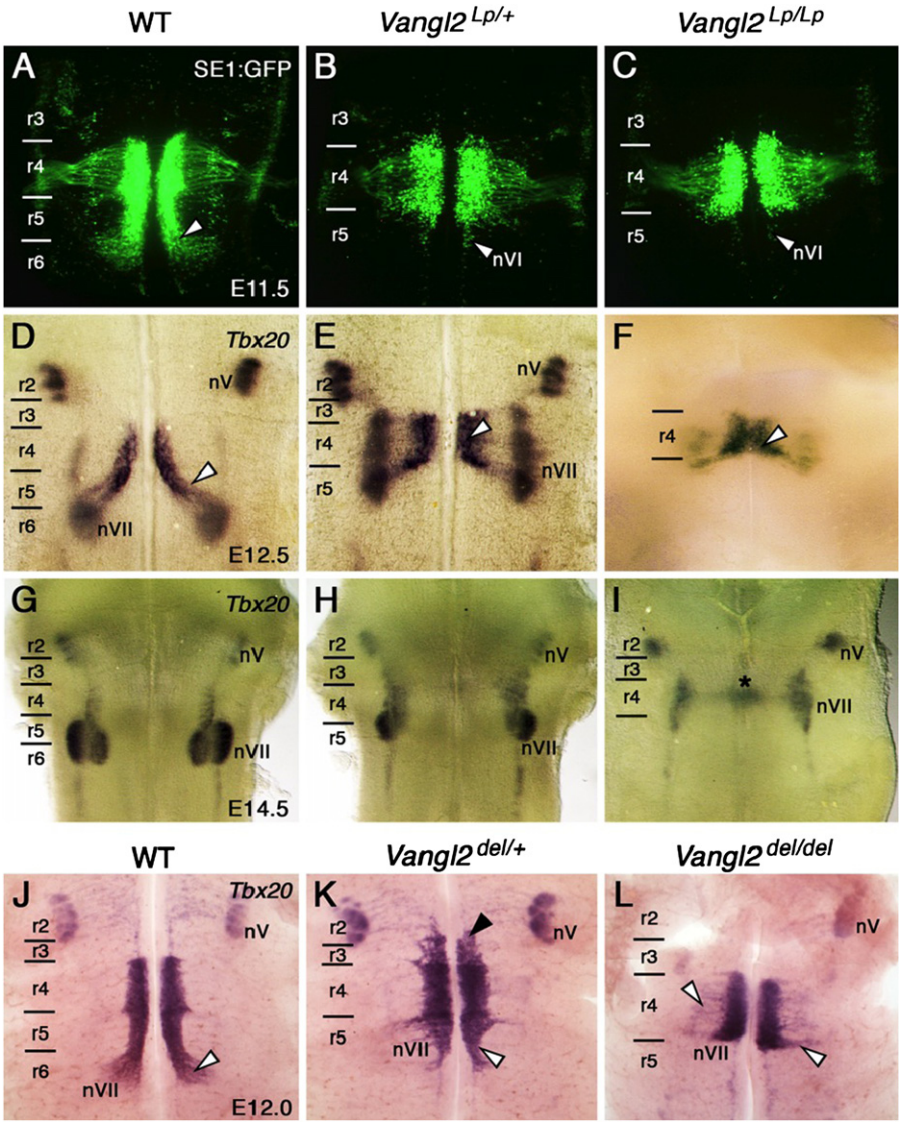

Fig. 2. FBM neurons fail to migrate caudally in *looptail* mutants and *Vangl2* knockout embryos. The trigeminal motor nucleus (nV) is located in r2 in all embryos. (A)–(C), Ventricular views of *SE1::gfp* hindbrains. In a WT embryo (A), FBM neurons (white arrowhead) migrate caudally from r4 into r6 and radially away from the midline. In *Vangl2*$^{Lp/+}$ (B) and *Vangl2*$^{Lp/Lp}$ embryos (C), FBM neurons fail to migrate out of r4. GFP-expressing cells in r5 are abducens motor neurons (nVI; white arrowheads). (D)–(F), Ventricular views of hindbrains processed for *Tbx20* ISH. In a WT embryo (D), FBM neurons migrate caudally from r4 into r6 (white arrowhead), then migrate radially to form the facial motor nucleus (nVII) in r6. In *Vangl2*$^{Lp/+}$ embryos (E), most *Tbx20*-expressing cells remain in r4 in medial and lateral positions, reflecting a near-failure of caudal migration. In *Vangl2*$^{Lp/Lp}$ embryos (F), caudal migration is completely abolished, with all FBM neurons located medially within r4. The apparent fusion of FBM populations across the midline may result from the defective floorplate and open neural tube in mutants. (G)–(I), Pial views. In a WT embryo (G), FBM neurons have completed migration into r5/r6 to form the facial motor nucleus (nVII). In *Vangl2*$^{Lp/+}$ embryos (H), the facial motor nucleus (nVII) is elongated within r4/r5, and is confined entirely to r4 in *Vangl2*$^{Lp/Lp}$ embryos (I), with some fused clusters (asterisk) at the midline. (J) and (K), ventricular views of hindbrains processed for *Tbx20* ISH. In a WT embryo (J), FBM neurons (white arrowhead) migrate in characteristic fashion. In a *Vangl2*$^{del/+}$ embryo (K), FBM neurons span r3 (black arrowhead) to r5 (white arrowhead), and do not migrate into r6, with most of the neurons confined to r4. In a *Vangl2*$^{del/del}$ embryo (L), FBM neurons do not migrate out of r4, with some cells migrating radially within r4 (white arrowheads).

Vangl2$^{Lp/Lp}$, but not *Vangl2*$^{Lp/+}$ embryos (Murdoch et al., 2001; Torban et al., 2004b; Ybot-Gonzalez et al., 2007), the failure of FBM neurons to migrate caudally in *looptail* mutants is not a secondary consequence of neural tube defects (Table S1).

The failure of FBM neuron migration in *Vangl2*$^{Lp/+}$ embryos may reflect a dominant negative nature of the *Vangl2*^{Lp} allele, which encodes a protein that fails to reach the plasma membrane (Iliescu et al., 2011; Torban et al., 2007). Therefore, we also examined FBM neuron migration in *Vangl2* knockout mice (*Vangl2*$^{del/del}$), where no Vangl2 protein is detected (Song et al., 2010). No FBM neurons migrated caudally in *Vangl2*$^{del/del}$ embryos (Fig. 2L; $n=5$). While a significant number of FBM neurons migrated caudally in *Vangl2*$^{del/+}$ embryos and formed a facial motor nucleus in r6, a large number of neurons also failed to migrate out of r4 (Fig. 2K; data not shown; $n=11$). In a few *Vangl2*$^{del/+}$ embryos (3/11), *Tbx20*+ve cells were found in r3 and r2 (Fig. 2K) suggestive of aberrant rostral migration (Table S1). Together, the *Vangl2*$^{Lp/+}$ and *Vangl2*$^{del/+}$ phenotypes suggest that the caudal migration defects in these embryos result from haploinsufficiency.

FBM neurons are specified and differentiate normally in Vangl2^{Lp} *mutants*

We tested whether the FBM migration defects in *Vangl2*^{Lp} mutants were a consequence of improper progenitor specification. *Math3* and *Mash1* encode transcription factors essential for FBM progenitor specification and their subsequent migration, and

are expressed in longitudinal domains in the ventricular zone (Ohsawa et al., 2005; Tiveron et al., 2003). These expression domains were not affected in *Vangl2*$^{Lp/+}$ and *Vangl2*$^{Lp/Lp}$ embryos (Fig. 3B–F; *Math3*: *Lp*/+ (n=3), *Lp*/*Lp* (2); *Mash1*: *Lp*/+ (2), *Lp*/*Lp* (2)), indicating that mutant FBM neurons are specified correctly. Furthermore, FBM neurons in both WT and *Vangl2*^{Lp} mutants expressed *Phox2b*, another branchiomotor and visceromotor differentiation marker (Pattyn et al., 2000), indicating that the non-migrating cells in the *Vangl2*^{Lp} mutants differentiate normally (Fig. S3A–C; WT (n=8), *Lp*/+ (7), *Lp*/*Lp* (3)). Interestingly, *Ret7*, a GDNF receptor that is normally expressed by FBM neurons in r6 (Garel et al., 2000), was expressed by non-migrated neurons in r4 of *Vangl2*$^{Lp/+}$ and *Vangl2*$^{Lp/Lp}$ embryos (Fig. S3H, I; WT (n=3), *Lp*/+ (4), *Lp*/*Lp* (2)), suggesting that the entire program of FBM neuron differentiation proceeds normally in the absence of caudal migration.

Immunostaining of peripheral nerves with a neurofilament antibody (NF160) revealed similar projection patterns for the trigeminal (nV) and facial (nVII) nerves in E11.5 embryos of all genotypes (Fig. 3G–I; WT (n=2), *Lp*/+ (3), *Lp*/*Lp* (2)), indicating that despite a failure of FBM neurons to migrate, their axons project and branch correctly, and innervate peripheral targets in mutant embryos. To investigate this further, we applied NeuroVue dyes (Fritzsch et al., 2005) in the second branchial arch to retrogradely label FBM neuron cell bodies through their axonal projections. Consistent with NF160 staining, FBM neurons were found in r4 in *Vangl2*$^{Lp/+}$ and *Vangl2*$^{Lp/Lp}$ mutants, although they were reduced in number in the latter (Fig. S3D–F; *Lp*/+ (n=3), *Lp*/*Lp* (2)). This reduction may result from open neural tube defects in *Vangl2*$^{Lp/Lp}$ embryos rather than due to failure of caudal migration, since the numbers of back-filled FBM neurons were qualitatively similar in wild-type and *Vangl2*$^{Lp/+}$ embryos even though caudal migration was nearly absent in heterozygotes (Fig. S3D, E).

Finally, we investigated whether the *Vangl2*^{Lp} mutation affected the development of other neuronal types in the r4–r5 region. The rhombomere markers *Hoxb1* (r4) and *Krox20* (r3/r5) were expressed normally in *Vangl2*$^{Lp/+}$ and *Vangl2*$^{Lp/Lp}$ embryos (see Fig. 1 in Thoby-Brisson et al., 2012), indicating that rhombomere patterning is not affected by the failure of the neural tube to close in *Vangl2*$^{Lp/Lp}$ mutants, and that FBM neuron migration defects are not due to defective hindbrain patterning. Rhombomere 4 generates both FBM and inner ear efferent (IEE) neurons. Whereas, FBM neurons migrate caudally out of r4, IEE neurons, which express *Gata3* (Karis et al., 2001), are confined to r4 (Fritzsch et al., 1993). In r5, the non-migratory abducens motor neurons express the somatomotor neuron marker *Hb9* (Thaler et al., 1999). In WT embryos, *Gata3* was found in a high-expressing medial domain adjacent to the floorplate and a weaker-expressing lateral domain, but not expressed in FBM neurons (Fig. S4A–A′; n=6). This expression pattern was not

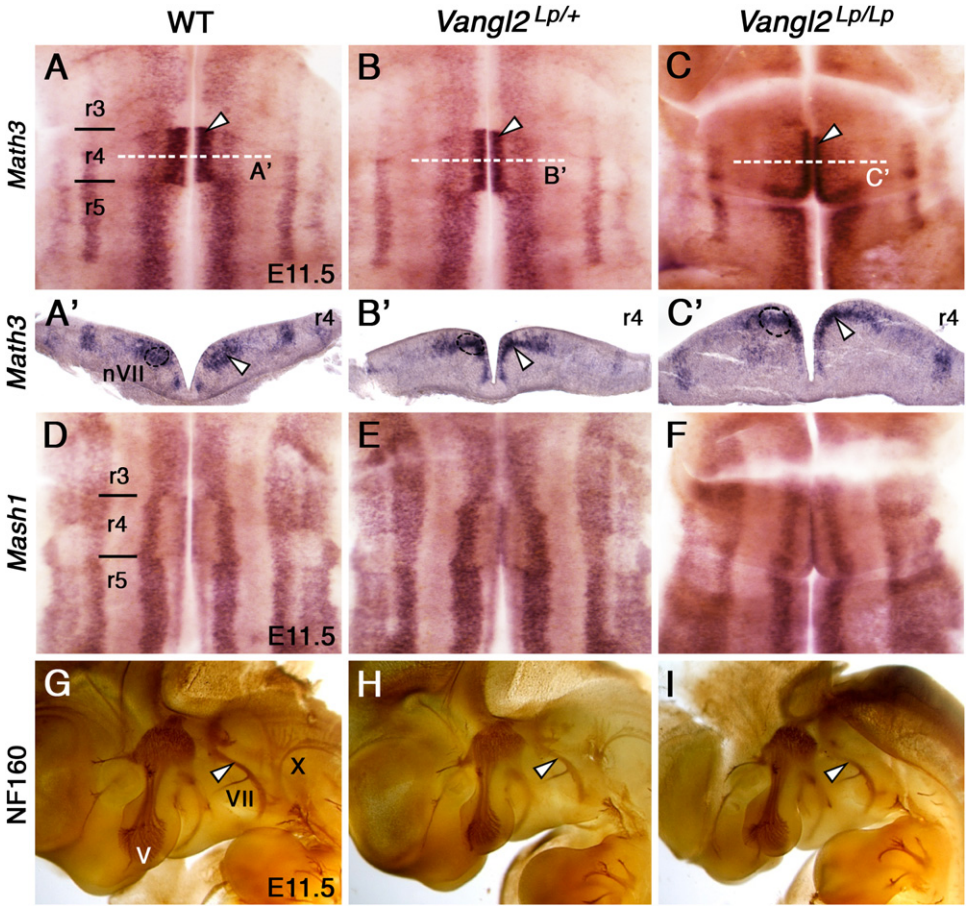

Fig. 3. Normal hindbrain development in *looptail* mutants. (A)–(F), ventricular views; (A′)–(C′), coronal sections. *Math3* expression in r4 (white arrowhead) is predominantly in the motor neuron progenitor domain (pMN, dotted circle) in WT (A) and (A′) embryos, and is unaffected in *Vangl2*$^{Lp/+}$ (B) and (B′) and *Vangl2*$^{Lp/Lp}$ (C) and (C′) embryos. *Mash1* expression in medial aspect of r4 is also limited to the pMN domain in the WT embryo (D), and is unaffected in *Vangl2*$^{Lp/+}$ (E), and *Vangl2*$^{Lp/Lp}$ (F) embryos. (G)–(I), Lateral views, rostral to the left, of NF160-stained embryos. In a WT embryo (G), the trigeminal (V) and facial (VII, white arrowhead) nerves project into the first and second branchial arches, respectively, and the vagus (X) nerve exits from the caudal hindbrain. These projections are essentially normal in *Vangl2*$^{Lp/+}$ (H) or *Vangl2*$^{Lp/Lp}$ (I) embryos.

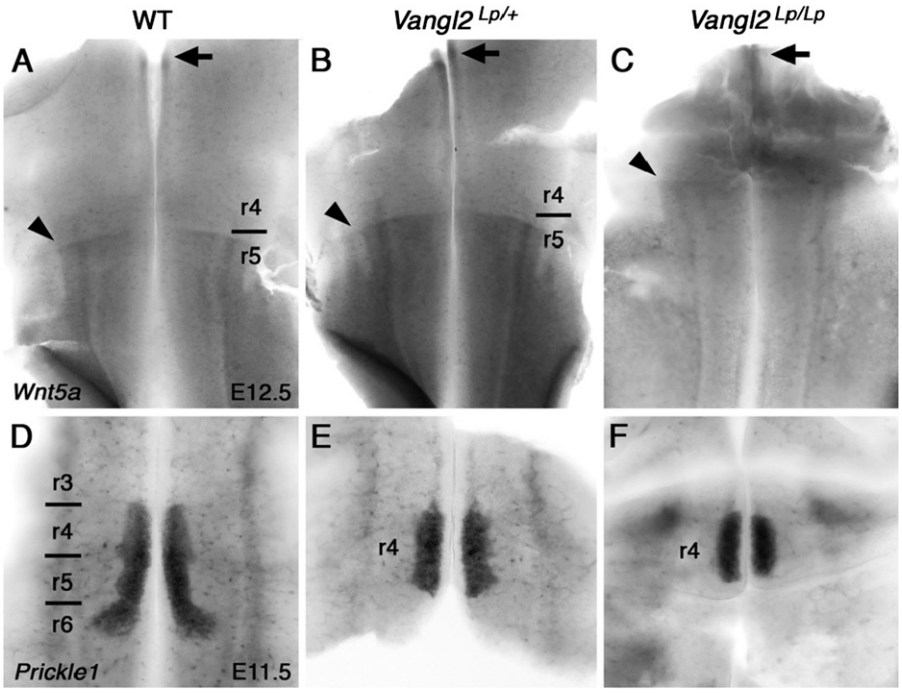

Fig. 4. Normal expression of Wnt/PCP genes in *looptail* mutants. In a WT embryo (A), *Wnt5a* is expressed in r5 and caudally, with a sharp r4/r5 boundary (black arrowhead). The rostral domain of *Wnt5a* expression (black arrow) extends into r3. *Wnt5a* expression is normal in *Vangl2*$^{Lp/+}$ embryos (B). In a *Vangl2*$^{Lp/Lp}$ embryo (C), *Wnt5a* expression is reduced, although a boundary and the medial expression domain (arrow) are intact despite neural tube defects. In a WT embryo (D), *Prickle1* is expressed in FBM neurons along their migratory route spanning r4 through r6. In *Vangl2*$^{Lp/+}$ (E) and *Vangl2*$^{Lp/Lp}$ (F) embryos, *Prickle1*-expressing FBM neurons are confined to r4.

affected in *Vangl2*$^{Lp/+}$ embryos (Fig. S4B–B′; *Lp*/+ (n=8)), and was slightly reduced in the r4 medial domain in *Vangl2*$^{Lp/Lp}$ embryos (Fig. S4C–C′; *Lp*/*Lp* (n=1)), correlating with the absence of *Tbx20*-expressing IEE neurons (Fig. S2C–C′). Importantly, however, *Gata3* was not expressed ectopically in FBM neurons (Fig. S4B and C′). Similarly, *Hb9* was not ectopically expressed in FBM neurons in r4 of *Vangl2*$^{Lp/+}$ and *Vangl2*$^{Lp/Lp}$ embryos (Fig. S4D–F; *Lp*/+ (n=10), *Lp*/*Lp* (5)). Together, these results indicate that the failure of FBM neurons to migrate caudally in *Vangl2*^{Lp} mutants is not due to a misspecification as non-migratory neurons.

Wnt/PCP genes are expressed normally in Vangl2^{Lp} *mutants*

In mouse *Tbx20* mutants, FBM neurons fail to migrate caudally and poorly express several Wnt/PCP genes, including *Vangl2*, *Prickle1* (*Pk1*) and *Wnt11* (Song et al., 2006). In zebrafish, *pk1b* is expressed in FBM neurons, and is necessary for caudal migration (Rohrschneider et al., 2007). In addition, *Wnt5a* is expressed in the vicinity of FBM neurons and may function as an attractive cue for caudal migration (Song et al., 2006; Vivancos et al., 2009). Therefore, we examined the expression of *Wnt5a* and *Pk1* in *Vangl2*^{Lp} mutants. In WT hindbrains, *Wnt5a* was expressed at the midline up to r3, then broadly in the neuroepithelium from r5 and caudally, with a sharp boundary at the r4/r5 border (Fig. 4A; n=4; Vivancos et al., 2009). In *Vangl2*$^{Lp/Lp}$ mutants (Fig. 4C; n=4), the boundary was less clear and overall expression levels appeared lower. However, *Wnt5a* expression in *Vangl2*$^{Lp/+}$ embryos (Fig. 4B; n=4), which have FBM migration defects, was indistinguishable from WT, indicating that the caudal migration defect in *Vangl2*$^{Lp/Lp}$ mutants is not due to altered *Wnt5a* expression. *Pk1* was expressed in FBM neurons in both WT and *Vangl2*^{Lp} mutants (Fig. 4D–F; WT (n=2), *Lp*/+ (2), *Lp*/*Lp* (2)). Together, these data suggest that defective FBM neuron migration in *Vangl2*^{Lp} mutants does not result from altered Wnt/PCP gene expression.

Ptk7, which interacts genetically with Vangl2, is necessary for FBM neuron migration

Ptk7 is a PCP gene encoding a transmembrane, tyrosine kinase-like protein (Mossie et al., 1995) that genetically interacts with *Vangl2* during PCP events like neural tube closure and stereociliary bundle orientation in the inner ear (Lu et al., 2004; Paudyal et al., 2010). Therefore, we examined FBM neuron migration in the mouse *Ptk7* mutant *chuzhoi* (*chz*), in which the level of soluble Ptk7 is greatly reduced (Paudyal et al., 2010). In E12.5 *Ptk7*$^{chz/chz}$ mutants (n=6), *Tbx20* in situ showed that most FBM neurons failed to migrate caudally out of r4 (Fig. 5). In some embryos (4/6), a few FBM neurons migrated caudally to a similar extent as WT (compare Fig. 5C to 5A). By E14.5, FBM neurons had completed dorso-lateral migration to form the facial motor nucleus (nVII) near the pial surface in r6 of WT and *Ptk7*$^{chz/+}$ embryos (Fig. 5D and E; WT (n=8), *chz*/+ (7)), and in r4 of *Ptk7*$^{chz/chz}$ embryos (Fig. 5F; n=8), demonstrating a clear role for *Ptk7* in caudal, but not dorso-lateral, migration of FBM neurons in mice.

Dishevelled function is dispensable for caudal migration of FBM neurons

In mice, Wnt5a and Wnt7a can act as chemoattractants for FBM neurons in an explant assay; however, their in vivo roles are less clear since FBM neurons migrate caudally out of r4 in *Wnt5a* and *Wnt7a* mutants, with a slight defect in dorso-lateral migration in r5/r6 in *Wnt5a* mutants (Vivancos et al., 2009). In zebrafish, several Wnt/PCP genes (*vangl2*, *pk1a*, *pk1b*, *fzd3a*, *celsr1-3*, *scrib*) are necessary for FBM neuron migration (Bingham et al., 2002; Carreira-Barbosa et al., 2003; Jessen et al., 2002; Rohrschneider et al., 2007; Wada et al., 2005, 2006), but *wnt5b* and *wnt11* appear to be dispensable (Jessen et al., 2002). Importantly, over-expression of *Xdd1* (Sokol, 1996), a dominant negative form of *Dishevelled* (*Dvl*), the central downstream

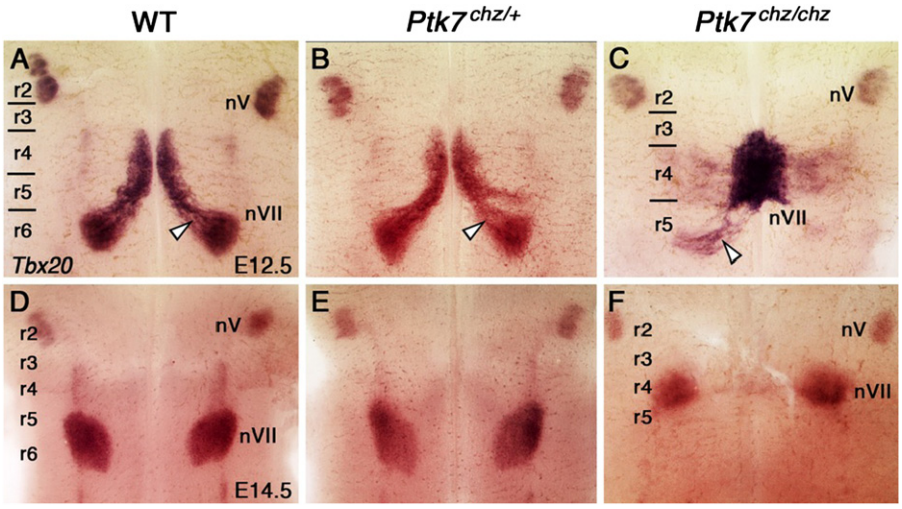

Fig. 5. FBM neurons fail to migrate caudally in *chuzhoi* mutants. Ventricular (A)–(C) and pial (D)–(F) views of embryos processed for *Tbx20* ISH. In E12.5 WT (A) and $Ptk7^{chz/+}$ (B) embryos, FBM neurons migrate caudally from r4 into r6 (arrowheads) to form the facial motor nucleus (nVII). In $Ptk7^{chz/chz}$ mutants (C), FBM neurons completely or largely fail to migrate out of r4, with a few neurons migrating caudally into r5 (white arrowhead). By E14.5, FBM neurons in WT (D) and $Ptk7^{chz/+}$ (E) embryos have completed their caudal and radial migrations to form facial motor nuclei (nVII) in r6. In $Ptk7^{chz/chz}$ mutants (F), the facial motor nuclei are rostrally displaced and located in r4 (8/8 embryos). The location of the trigeminal motor neurons (nV) in r2 is not affected in mutants.

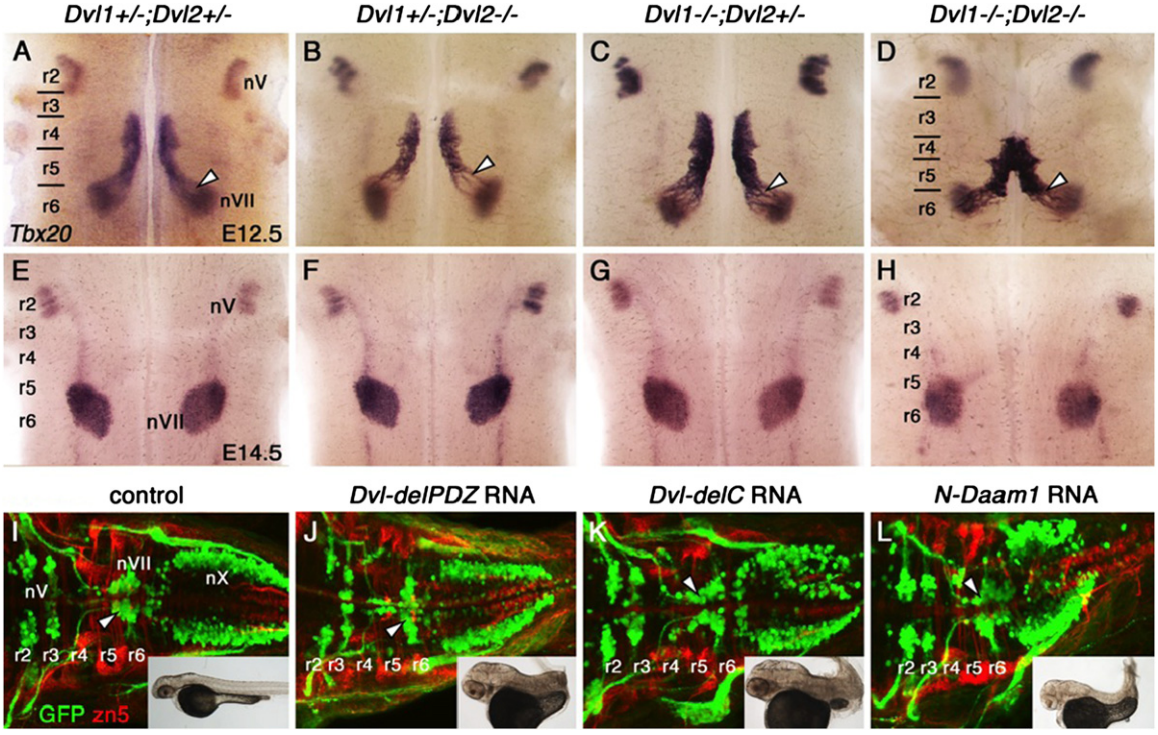

Fig. 6. Caudal migration of FBM neurons is not affected by loss of Dishevelled function. Ventricular (A)–(D) and pial (E)–(H) views of embryos processed for *Tbx20* ISH. In E12.5 control *Dvl1+/-;Dvl2+/-* embryos (A), FBM neurons migrate caudally from r4 into r6 (arrowhead) to form the facial motor nucleus (nVII). This caudal migration occurs normally in *Dvl1+/−;Dvl2−/−* (B), *Dvl1−/-;Dvl2+/−* (C), and *Dvl1−/−;Dvl2−/−* mutants (D), inspite of neural tube closure defects in many of these embryos. By E14.5, FBM neurons in control embryos (E) have completed their caudal and radial migrations to form facial motor nuclei (nVII) in r6. Likewise, these nuclei are formed in r6 in *Dvl*-deficient embryos including *Dvl1+/−;Dvl2−/−* (F, 2/2 embryos), *Dvl1−/−;Dvl2+/−* (G, 6/6 embryos), and *Dvl1−/−;Dvl2−/−* mutants (H, 4/4 embryos). Neural tube defects were seen in *Dvl1−/−;Dvl2−/−* mutants. I-L, Dorsal views of 48 hpf *Tg(isl1:gfp)* zebrafish embryos processed for anti-GFP and zn5 immunohistochemistry. In control embryos (I), GFP-expressing FBM neurons migrate caudally from r4 into r6 (arrowhead) and r7 to form the facial motor nucleus (nVII). Zn5 staining labels rhombomere boundaries. The trigeminal (nV) and vagal (nX) motor neurons are located in r2 and r3, and the caudal hindbrain, respectively. Inset shows intact embryo with normal extension of the body axis. In embryos injected with *Dvl-delPDZ* (J), *Dvl-delC* (K), and *N-Daam1* (L) RNA (200 pg/embryo), FBM neurons are able to migrate caudally (arrowheads) out of r4 despite convergence and extension defects resulting in a shortened body axis (insets). Positions of the nV and nX neurons are not affected by these treatments.

signaling mediator of the Wnt/PCP pathway, has no effect on caudal migration of FBM neurons (Jessen et al., 2002). To test directly a role for *Dvl* function in mice, we examined FBM neuron migration in *Dvl* knockout mice (Etheridge et al., 2008; Hamblet et al., 2002; Wang et al., 2005).

E12.5 and E14.5 embryos from *Dvl1+/−; Dvl2+/−* incrosses were collected and processed for *Tbx20* in situ. Combinatorial deletion of multiple copies of *Dvl1* and *Dvl2* did not disrupt caudal migration of FBM neurons (E12.5: Fig. 6A–C; E14.5: Fig. 6E–G), even in *Dvl1+/−; Dvl2−/−*embryos ($n=6$), some of which

exhibit hindbrain neural tube defects (3/6). Importantly, FBM neurons also migrated caudally into r6 in *Dvl1/2* double mutants (Fig. 6D and H; $n=4$ for each age), which exhibit profound PCP defects including a fully open neural tube and misorientation of stereociliary bundles (Etheridge et al., 2008; Hamblet et al., 2002; Wang et al., 2005; Table S1). Similar to *Vangl2*$^{Lp/Lp}$, FBM neurons in r4 of double mutants were initially fused at the midline (Fig. 6D). By E14.5, however, no *Tbx20*-expressing cells were found at the midline, and a well-defined facial motor nucleus was formed in r6 (Fig. 6H) indicating that FBM neurons undergo essentially normal caudal and radial (dorso-lateral) migrations in *Dvl1*; *Dvl2* double knockout embryos. Since three *Dvl* genes (1–3) are expressed in partially overlapping patterns in the mouse embryo (Tissir and Goffinet, 2006), *Dvl3* could potentially compensate for loss of *Dvl1/2* function in FBM neurons in double mutants. However, *Dvl3* expression is not affected in double mutants, and is restricted to the ventricular zone adjacent to the migrating FBM neurons at E12.5 (Fig. S5B; $n=2$) and post-migrated neurons at E14.5 (Fig. S5D; $n=1$). These results suggest strongly that caudal migration does not require *Dvl* function in FBM neurons.

Our previous studies with a dominant negative Dishevelled construct (*Xdd1*) in zebrafish embryos also suggested that FBM neuron migration is *Dvl*-independent (Jessen et al., 2002). To further validate these findings, we interfered with Dvl signaling using additional constructs, and examined their effects on caudal migration of FBM neurons using *Tg*(*isl1:gfp*) zebrafish embryos, which express GFP in branchiomotor neurons (Higashijima et al., 2000). Western blot analysis confirmed the presence of mutant proteins in 20 hpf embryos during the period of neuronal migration (Fig. S6B). For embryos injected with *Dvl-delPDZ* RNA, we confirmed by whole-mount immunostaining the presence of myc-tagged protein both in the motor neurons and in adjacent cells (Fig. S6C). Similar to mice, zebrafish FBM neurons are born in r4 and migrate caudally into r6 and r7 (Fig. 6I; Chandrasekhar, 2004; Chandrasekhar et al., 1997; Higashijima et al., 2000). While over-expression of the dominant negative *Dvl* construct (*Xdd1/Dvl-delPDZ*; Tada and Smith, 2000) generated convergence and extension (CE) defects during gastrulation as expected, resulting in a shortened body axis, caudal migration of FBM neurons was not affected (Fig. 6J; Jessen et al., 2002). Importantly, over-expression of additional dominant negative constructs, *Dvl-delC* (lacking the DEP domain and C-terminal; Tada and Smith, 2000) and *N-Daam1* (lacking Formin-homology domains to bind Dvl and activate downstream signaling; Habas et al., 2001), generated CE defects, but failed to disrupt caudal FBM neuron migration (Fig. 6K and L; summarized in Fig. S6A). Since the dominant negative constructs would interfere with *Dvl*-mediated signaling notwithstanding the expression of multiple *Dvl* genes, these data suggest strongly that caudal migration of FBM neurons does not require Dishevelled function.

Since FBM neuron migration is *Vangl2*-dependent (Fig. 2), and Vangl2 and Dvl physically interact (Torban et al., 2004b), we further tested a potential role for Dvl function in migration by examining whether *Dvl2* and *Vangl2* interact genetically for this process. It was demonstrated previously that *Dvl2* and *Vangl2*^{Lp} interact genetically during neurulation, with *Vangl2*$^{Lp/+}$; *Dvl2*−/− embryos showing craniorachischisis while *Vangl2*$^{Lp/+}$; *Dvl2*+/− embryos have closed neural tubes (Wang et al., 2006). Therefore, we tested whether a reduction in Dvl signaling by lowering *Dvl2* copy number exacerbated the FBM migration defect of *Vangl2*$^{Lp/+}$ embryos. Removal of one or both copies of *Dvl2* in a *Vangl2*$^{+/+}$ background had no effect on migration of FBM neurons out of r4 (Fig. 7B and C; *Dvl2*+/− ($n=14$), *Dvl2*−/− (14); pooled data), although *Dvl2*−/− mice exhibited mild PCP defects (Hamblet et al., 2002). Importantly, many FBM neurons migrated in thick streams into r5 in both *Vangl2*$^{Lp/+}$; *Dvl2*+/− (5/5 embryos; Fig. 7E) and *Vangl2*$^{Lp/+}$; *Dvl2*−/− embryos (5/5 embryos; Fig. 7F), similar to the phenotype of *Vangl2*$^{Lp/+}$ embryos (Fig. 7D; $n=4$), suggesting that *Vangl2* and *Dvl2* do not genetically interact to regulate caudal FBM neuron migration. Since *Vangl2*$^{Lp/+}$; *Dvl2*−/− embryos had fully open neural tubes (Wang et al., 2006; data not shown), the clusters of non-migrated FBM neurons in r4 were fused across the midline (Fig. 7F), as in *Vangl2*$^{Lp/Lp}$ (Fig. 7G) and *Dvl1*−/−; *Dvl2*−/− embryos (Fig. 6D), giving the appearance of a stronger migration defect than in *Vangl2*$^{Lp/+}$; *Dvl2*+/− embryos (Fig. 7E). Interestingly, putative

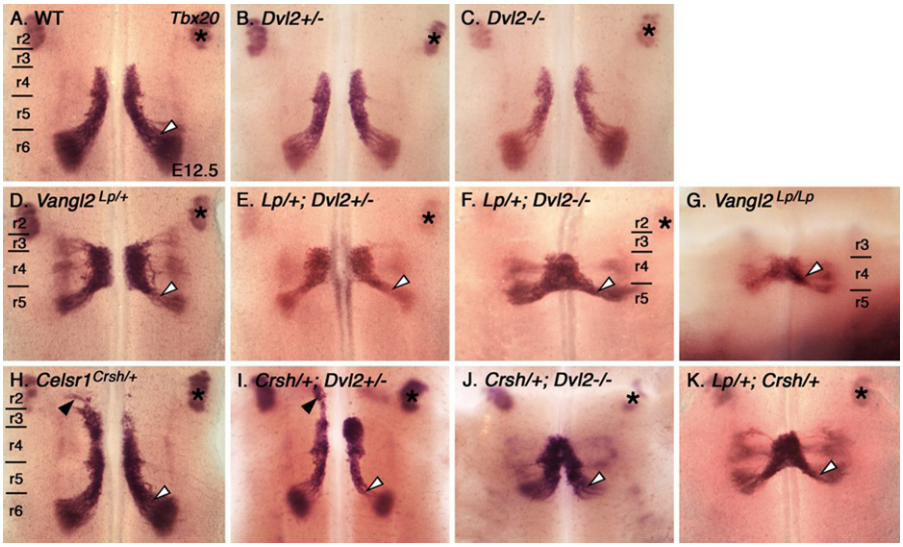

Fig. 7. Genetic interactions between *Vangl2*^{Lp}, *Dvl2*, and *Celsr1*^{Crsh} for FBM neuron migration. The caudal migratory streams of FBM neurons are labeled with white arrowheads, while rostrally-migrating neurons in *Celsr1*-deficient embryos are labeled with black arrowheads. The location of the trigeminal (nV) motor nucleus (demarcating r2) is noted with an asterisk in every preparation except G. (A)–(C), Removing *Dvl2* genes from a wild-type background (A) did not affect FBM neuron migration (B) and (C). (D)–(F), Removing *Dvl2* genes from a *Vangl2*$^{Lp/+}$ background (D), did not exacerbate the migration defect of *Vangl2*$^{Lp/+}$ embryos, with thick streams of FBM neurons migrating caudally into r5 (E) and (F), compared to *Vangl2*$^{Lp/Lp}$ embryos (G). Fusion of FBM clusters across the midline may be a consequence of defects in neural tube and floorplate development in these embryos. (H)–(J), While removing one copy of *Dvl2* had no effect on the abnormal rostral migration of FBM neurons (black arrowhead, I), as seen in *Celsr1*$^{Crsh/+}$ embryos (H), removing the second copy of *Dvl2* completely blocked rostral migration (J), but not caudal migration. Rostral migration was also blocked in *Vangl2*$^{Lp/+}$; *Celsr1*$^{Crsh/+}$ embryos (K).

migration of FBM neurons into r3, noted in some *Vangl2*$^{Lp/+}$ embryos (Fig. 7D; 3/4), was never seen in *Vangl2*$^{Lp/+}$; *Dvl2*−/− embryos, suggesting that the ectopic migration may be *Dvl*-dependent.

To test this possibility, we crossed *Dvl2* mutants with *Crash* mice, which carry a mutation in an extracellular cadherin repeat of the atypical cadherin *Celsr1* (Torban et al., 2007) that results in a subset of FBM neurons migrating rostrally into r2 and r3 (Qu et al., 2010). In *Celsr1*$^{Crsh/+}$ embryos, a significant number of FBM neurons migrated rostrally into r2/r3, although most migrated caudally into r6 (Fig. 7H; $n=13$; Table S1; Qu et al., 2010). Importantly, while many FBM neurons migrated rostrally in *Celsr1*$^{Crsh/+}$; *Dvl2*+/− embryos (Fig. 7I; 12/14), this defect was completely suppressed in *Celsr1*$^{Crsh/+}$; *Dvl2*−/− embryos (Fig. 7J; $n=5$). These data suggest that while caudal FBM neuron migration is likely independent of *Dvl* activity, the aberrant rostral migration seen in *Celsr1*$^{Crsh/+}$ embryos requires *Dvl* function. Finally, the rostral migration defect was also suppressed in *Vangl2*$^{Lp/+}$; *Celsr1*$^{Crsh/+}$ transheterozygotes (Fig. 7K; $n=3$; Table S1), indicating further that aberrant rostral migration is a response to Wnt/PCP signaling since it is sensitive to reduction in both *Dvl* and *Vangl2* function.

Discussion

Our detailed characterization of FBM neuron migration defects in looptail mutants has highlighted the specificity of the phenotype within the hindbrain. We have shown that the failure of motor neuron migration is not a result of defective specification or differentiation of the neurons. Moreover, expression of some Wnt/PCP genes is not affected in mutants. Importantly, we find that caudal migration of FBM neurons is insensitive to severe reduction of Dishevelled function, suggesting that this mode of migration may be independent of Wnt/PCP signaling (Fig. 8).

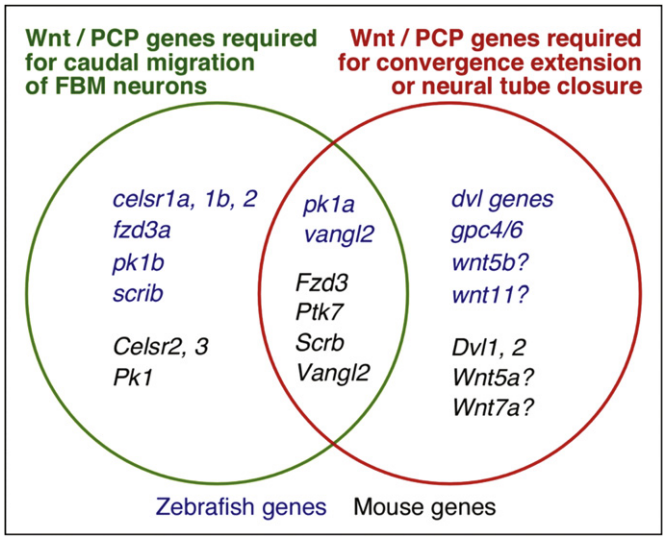

Fig. 8. Differential roles for Wnt/PCP genes in regulating FBM neuron migration and neural tube morphogenesis. Mouse (black) and zebrafish (blue) Wnt/PCP genes are categorized based on their roles in regulating caudal migration of FBM neurons or hallmark PCP processes like convergence and extension movements during gastrulation (zebrafish) and neural tube closure (mouse). These data are based on the phenotypes of mouse mutants and zebrafish mutants or morphants, with the exception of zebrafish *Dvl* genes, which were tested using dominant-negative reagents. The "?"s after the Wnt genes signify that double mutants have not been tested, so a putative role in FBM migration cannot be ruled out. Zebrafish data from Wada et al., 2006 (*celsr1a, 1b, 2, fzd3a*), Mapp et al., 2010, 2011 (*pk1b*), Wada et al., 2005 (*scrib*), Carreira-Barbosa et al., 2003 (*pk1a*), Jessen et al., 2002 (*vangl2*, *wnt5b*, *wnt11*), Bingham et al., 2002 (*gpc4/6*), and this report (*dvl* genes). Mouse data from Vivancos et al., 2009 (*Vangl2*, *Fzd3*, *Scrb*, *Wnt5a*, *Wnt7a*), Qu et al., 2010 (*Celsr2*, *3*, *Fzd3*), and this report (*Vangl2*, *Ptk7*, *Dvl1*, *2*). Mouse *Pk1* knockout phenotype (B. Fritzsch, personal communication).

Effects of Vangl2 mutations on FBM neuron migration and PCP events

In both *Vangl2*$^{del/+}$ and *Vangl2*$^{Lp/+}$ embryos, most FBM neurons fail to migrate caudally, a fully penetrant phenotype for both alleles. Since no *Vangl2* protein is detected in *Vangl2*$^{del/del}$ mice (Song et al., 2010), the *Vangl2*$^{del/+}$ phenotype is likely due to haploinsufficiency, with a high level of *Vangl2* activity required for caudal FBM neuron migration. The *Vangl2*$^{Lp/+}$ migration phenotype also results from reduction of *Vangl2* activity, because the *Vangl2*^{Lp} allele encodes either a non-functional or a dominant negative protein. Some studies suggest that the *Vangl2*^{Lp} allele is null because the mutant protein fails to reach the plasma membrane (Iliescu et al., 2011; Merte et al., 2010; Torban et al., 2007) and is unlikely to compete with WT *Vangl2* for intracellular binding partners, especially since mutant *Vangl2* does not bind *Dvl* in vitro (Torban et al., 2004b). Other studies suggest that the *Vangl2*^{Lp} allele is dominant negative since the mutant protein decreases wild-type *Vangl2* phosphorylation, which is essential for its function (Gao et al., 2011; Song et al., 2010). Nonetheless, regardless of the nature of the *Vangl2*^{Lp} allele, FBM neurons largely fail to migrate caudally in *Vangl2*$^{Lp/+}$ embryos suggesting that FBM neuron migration is quite sensitive to the level of *Vangl2* function. Similar migration defects were noted in *Vangl2*$^{Lp/+}$ embryos in a previous study (Vivancos et al., 2009) using a different *Lp* allele (S464N; Murdoch et al., 2001), consistent with a dose-dependent role for Vangl2 in this process. Interestingly, no defects in caudal migration were seen in zebrafish embryos heterozygous for either of two mutations in *vangl2* (*trilobite* alleles: *tri* ^{tk50f} and *tri* ^{tc240a}; Bingham et al., 2002) including one that results in no detectable transcript (*tri* ^{tk50f}; Jessen et al., 2002). However, since biochemical or genetic compensatory mechanisms cannot be ruled out to explain the zebrafish data, we favor the idea that high levels of Vangl2 activity are required for caudal migration of FBM neurons.

Although some PCP events like stereocilia orientation are affected in *Vangl2*$^{Lp/+}$ and *Vangl2*$^{del/+}$ embryos (Montcouquiol et al., 2006; Song et al., 2010), other PCP processes are not affected since both *Vangl2*$^{del/+}$ and *Vangl2*$^{Lp/+}$ embryos have normal, closed neural tubes. Importantly, however, both exhibit strong and comparable caudal migration defects (Table S1). If one assumes that Vangl2 regulates FBM neuron migration and PCP processes through the same molecular pathways, these data suggest that FBM neuron migration is more sensitive to levels of Vangl2 than neural tube closure. Alternatively, Vangl2 may perform unique and separable functions, acting through independent pathways, for neuronal migration and neural tube closure, since these cellular processes have been uncoupled in *Vangl2* heterozygotes.

Site of Vangl2 function for FBM neuron migration

In zebrafish embryos, *vangl2* is expressed ubiquitously in the neural tube and non-neural tissues at the onset and early stages of FBM neuron migration (Jessen and Solnica-Krezel, 2004; Park and Moon, 2002). Genetic mosaic analysis with zebrafish *trilobite* mutants indicates that *vangl2* functions primarily in a non-cell autonomous manner to regulate FBM neuron migration (Jessen et al., 2002; Walsh et al., 2011). In contrast to zebrafish, mouse *Vangl2* expression in the hindbrain is restricted to the ventricular zone and to differentiating FBM neurons (Song et al., 2006; Fig. 1).

Therefore, it is possible that *Vangl2* functions within FBM neurons in mice. Consistent with this idea, conditional inactivation of *Tbx20* in facial motor neurons leads to the failure of caudal migration, concomitant with the loss of *Vangl2* expression in these neurons (Song et al., 2006).

Alternatively, *Vangl2* may function non-cell autonomously in mice, as in zebrafish, to regulate FBM neuron migration. Cell transplantation experiments in zebrafish indicate a role for *vangl2* in floorplate cells for neuronal migration, and FBM neurons fail to migrate out of r4 in a mouse mutant lacking floorplate cells (Sittaramane, V., Glasco, D. et al., in preparation). Since *Vangl2* is transiently expressed in mouse floorplate cells between E9.5-10.5, prior to FBM neuron migration, we cannot rule out a floorplate-associated role for *Vangl2* in this process. The role of *Vangl2* in specific hindbrain cell types can be addressed by generating tissue-specific knockouts using the $Vangl2^{flox}$ allele (Song et al., 2010).

In zebrafish, FBM neurons use the laminin-expressing basement membrane as a substrate for their caudal migration from r4 to r6/r7 (Grant and Moens, 2010). In contrast, mouse FBM neurons migrate caudally in close proximity to the ventricular zone from r4 into r6, where they migrate radially to the pial surface. Interestingly, *Lamininα5* is expressed along the ventricular zone in the mouse hindbrain (Coles et al., 2006), whereas in zebrafish, laminins are restricted to the basement membrane (Grant and Moens, 2010). The hindbrain expression domains of mouse *Lamininα5*, *Vangl2* and *Celsr1* overlap, and in zebrafish, *lamininα1* genetically interacts with *vangl2* to regulate FBM neuron migration (Sittaramane et al., 2009). Therefore, it is possible that Vangl2 and Celsr1 interact with Laminins and other molecules at the ventricular surface of the mouse hindbrain to guide the caudal migration of FBM neurons.

Caudal migration of FBM neurons may be independent of Wnt/PCP and Dishevelled signaling

FBM neuron migration defects have been described in multiple Wnt/PCP mutants in both mice and zebrafish (Bingham et al., 2002; Carreira-Barbosa et al., 2003; Mapp et al., 2010; Qu et al., 2010; Vivancos et al., 2009; Wada et al., 2005, 2006). However, it is unclear whether FBM neuron migration is a PCP-dependent process. Our finding that caudal FBM neuron migration is blocked in *Ptk7* mutants is consistent with a role for Wnt/PCP signaling since *Ptk7* genetically interacts with *Vangl2*, and is a regulator of PCP signaling (Lu et al., 2004; Paudyal et al., 2010). Furthermore, *Wnt5a* is expressed in a graded fashion from r5 and caudally, suggesting that it may act as an attractive cue to migrating FBM neurons (Vivancos et al., 2009). In hindbrain explant cultures, some FBM neurons migrate towards Wnt-coated beads. However, *Wnt5a* mutant embryos show only very minor defects in caudal FBM neuron migration and *Wnt7a* mutants show no migration defects. These observations suggest that Wnts (and PCP signaling) may play a minor or redundant role in regulating FBM neuron migration (Vivancos et al., 2009). Interestingly, mosaic analyses of *vangl2*, *scrib*, *pk1b*, and *Nancy-Horan syndrome-like 1b* (*nhsl1b*) in particular host environments have uncovered PCP-dependent and PCP-independent mechanisms underlying FBM neuron migration (Walsh et al., 2011).

To directly test the role of PCP signaling in FBM neuron migration, we examined *Dishevelled*-deficient embryos. FBM neurons migrate normally in *Dvl1|2* double mutants despite a fully open neural tube, a hallmark PCP defect (Table S1). This suggests either that FBM neuron migration and PCP events such as neural tube closure are regulated independently, or that caudal neuronal migration requires relatively *low* levels of Dvl/PCP signaling. Although mice express three *Dvl* genes in partially overlapping patterns (Tissir and Goffinet, 2006), *Dvl3* expression is not affected in *Dvl1|2* double mutants, and is excluded from FBM neurons (Fig. S6), suggesting strongly that caudal migration does not require *Dvl* function within FBM neurons. However, we cannot rule out that *Dvl3* compensates for loss of *Dvl1-2* function in *Dvl1|2* double mutants by acting non-autonomously during neuronal migration. Since *Dvl2|3* double mutants die by E9.5, prior to FBM neuron migration (Etheridge et al., 2008), testing a putative role for low-level, non-autonomous Dvl signaling in neuronal migration would necessitate generating triple mutants using conditional alleles. Importantly, however, disruption of *Dvl* signaling in zebrafish embryos with three different dominant-negative reagents generated only PCP defects (shortened body axis) and had no effect on FBM neuron migration. Since these constructs have the potential to interfere with the functions of multiple *Dvl* genes not only in motor neurons but also in surrounding tissues, our results suggest strongly that FBM neuron migration is independent of *Dvl* function (Fig. 8).

Whereas our *Dvl* data suggest that FBM neuron migration requires *lower* (or zero) levels of Dvl/PCP signaling (relative to that needed for neural tube closure), our $Vangl2^{Lp/+}$ data indicate that *higher* levels of PCP signaling are required (Table S1). Since these putative signaling requirements are mutually exclusive, we instead favor the model that FBM neuron migration and PCP processes are regulated independently of each other, with neuronal migration being independent of *Dvl* function. In this scenario, Vangl2 may possess a unique and separate function, not required for PCP, which acts in an alternate Dvl-independent pathway to regulate FBM neuron migration. Consistent with this idea, *vangl2* genetically interacts with non-PCP genes such as *tag1*, *lamininα1*, and *hdac1* to regulate FBM neuron migration in zebrafish (Nambiar et al., 2007; Sittaramane et al., 2009). Intriguingly, Vangl2 genetically and physically interacts with Pk1b (unpublished data cited in Mapp et al. (2010)), which is expressed in migrating FBM neurons (Rohrschneider et al., 2007), and regulates migration primarily through a novel PCP-independent pathway at the nucleus (Mapp et al., 2011).

Migration of FBM neurons at r3/r4 boundary is Dvl-dependent

Whereas the ability of FBM neurons to migrate caudally appears to be Dvl-independent, our data suggest that Dvl signaling must be reduced to prevent them from migrating rostrally into r3. We showed previously that in $Celsr1^{Crsh/+}$ mutants, a subset of FBM neurons migrates rostrally into r2/r3, though most FBM neurons migrate caudally into r6 (Qu et al., 2010). Since *Wnt5a* is also expressed along the midline in r2/r3 in addition to the caudal hindbrain (Fig. 4; Vivancos et al., 2009), we propose that mouse *Celsr1* normally functions to prevent FBM neurons at the r3/r4 boundary from migrating rostrally (in a Dvl-dependent manner) towards the chemoattractive Wnt5a source in r2/r3. Consistent with this, we found that loss of *Dvl2* function rescued the rostral migration defect in $Celsr1^{Crsh/+}$ embryos (Fig. 7). Similarly, loss of *Vangl2* function in $Celsr1^{Crsh/+}$ embryos ($Vangl2^{Lp/+}$; $Celsr1^{Crsh/+}$ transheterozygotes) also rescued the rostral migration defect (Fig. 7). Importantly, anterograde NeuroVue labeling experiments indicate that the FBM neurons migrating rostrally in $Celsr1^{Crsh/+}$ mutants originate exclusively from the r4 territory immediately adjacent to the r3/r4 boundary rather than from random or more caudal locations in r4 (D. Glasco and A. Chandrasekhar, unpublished observations). These results suggest that migration of FBM neurons at the r3/r4 boundary is especially sensitive to Dvl/Vangl2-dependent signaling, and that *Celsr1* function is necessary to block inappropriate rostral migration towards the Wnt5a source in r3. In contrast, migration of FBM neurons arising in the rest of r4 is either only weakly sensitive to or independent of Dvl signaling. This

model may also explain why FBM neurons are attracted to Wnt-coated beads placed laterally near the r3/r4 boundary (Vivancos et al., 2009), since FBM neurons at this boundary would be most sensitive to *Wnt*s, and free to migrate laterally toward the beads through a *Celsr1*-negative domain. Consistent with this model, *Wnt5a*-coated beads fail to attract FBM neurons in *Dvl2* mutants (W. Bryant, L. Reustle, and A. Chandrasekhar, unpublished observations). Thus, it appears that subsets of mouse FBM neurons may exhibit differential sensitivity to *Dvl* signaling depending upon their position within r4.

In conclusion, our work has defined a role for *Vangl2* in the caudal migration of FBM neurons that appears to be independent of PCP signaling mediated by Dishevelled. Our data also suggest that Wnt/PCP signaling can induce some FBM neurons to migrate rostrally but that this response is normally suppressed. It will be of interest to understand the mechanisms underlying the suppression of the rostral migration response, as well as the nature of the PCP-independent pathways regulating caudal migration.

Role of funding source

The funders played no role in study design, data collection and analysis, decision to publish, or preparation of the manuscript.

Acknowledgements

We thank members of the Chandrasekhar lab for discussion and fish care. We thank Olivier Pourquie and Sam Pfaff for the *looptail* and *SE1::gfp* mice, respectively. We thank Jane Johnson, Oni Mapp, Victoria Prince, Michelle Studer, Fadel Tissir, and Paul Trainor for probes and expression constructs. This work was supported by an NIH predoctoral fellowship 1F31NS063513 (DMG), the Bioimaging Research Center at GIST (MRS), the Medical Research Council (JNM), and NIH grant NS040449 (AC).

Appendix A. Supporting information

Supplementary data associated with this article can be found in the online version at http://dx.doi.org/10.1016/j.ydbio.2012.06.021.

References

Bingham, S., Higashijima, S., Okamoto, H., Chandrasekhar, A., 2002. The zebrafish trilobite gene is essential for tangential migration of branchiomotor neurons. Dev. Biol. 242, 149–160.

Carpenter, E.M., Goddard, J.M., Chisaka, O., Manley, N.R., Capecchi, M.R., 1993. Loss of Hox-A1 (Hox-1.6) function results in the reorganization of the murine hindbrain. Development 118, 1063–1075.

Carreira-Barbosa, F., Concha, M.L., Takeuchi, M., Ueno, N., Wilson, S.W., Tada, M., 2003. Prickle 1 regulates cell movements during gastrulation and neuronal migration in zebrafish. Development 130, 4037–4046.

Chandrasekhar, A., 2004. Turning heads: development of vertebrate branchiomotor neurons. Dev. Dyn. 229, 143–161.

Chandrasekhar, A., Moens, C.B., Warren Jr., J.T., Kimmel, C.B., Kuwada, J.Y., 1997. Development of branchiomotor neurons in zebrafish. Development 124, 2633–2644.

Coles, E.G., Gammill, L.S., Miner, J.H., Bronner-Fraser, M., 2006. Abnormalities in neural crest cell migration in laminin alpha5 mutant mice. Dev. Biol. 289, 218–228.

Coppola, E., Pattyn, A., Guthrie, S.C., Goridis, C., Studer, M., 2005. Reciprocal gene replacements reveal unique functions for Phox2 genes during neural differentiation. EMBO J. 24, 4392–4403.

Curtin, J.A., Quint, E., Tsipouri, V., Arkell, R.M., Cattanach, B., Copp, A.J., Henderson, D.J., Spurr, N., Stanier, P., Fisher, E.M., et al., 2003. Mutation of Celsr1 disrupts planar polarity of inner ear hair cells and causes severe neural tube defects in the mouse. Curr. Biol. 13, 1129–1133.

Darken, R.S., Scola, A.M., Rakeman, A.S., Das, G., Mlodzik, M., Wilson, P., 2002. The planar polarity gene strabismus regulates convergent extension movements in Xenopus. EMBO J. 21, 976–985.

Devenport, D., Fuchs, E., 2008. Planar polarization in embryonic epidermis orchestrates global asymmetric morphogenesis of hair follicles. Nat. Cell Biol. 10, 1257–1268.

Doudney, K., Stanier, P., 2005. Epithelial cell polarity genes are required for neural tube closure. Am. J. Med. Genet. C Semin. Med. Genet. 135, 42–47.

Etheridge, S.L., Ray, S., Li, S., Hamblet, N.S., Lijam, N., Tsang, M., Greer, J., Kardos, N., Wang, J., Sussman, D.J., et al., 2008. Murine Dishevelled 3 functions in redundant pathways with dishevelled 1 and 2 in normal cardiac outflow tract, cochlea, and neural tube development. PLoS Genet. 4, e1000259.

Fritzsch, B., Christensen, M.A., Nichols, D.H., 1993. Fiber pathways and positional changes in efferent perikarya of 2.5- to 7-day chick embryos as revealed with DiI and dextran amines. J. Neurobiol. 24, 1481–1499.

Fritzsch, B., Muirhead, K.A., Feng, F., Gray, B.D., Ohlsson-Wilhelm, B.M., 2005. Diffusion and imaging properties of three new lipophilic tracers, NeuroVue Maroon, NeuroVue Red and NeuroVue Green and their use for double and triple labeling of neuronal profile. Brain Res. Bull. 66, 249–258.

Gao, B., Song, H., Bishop, K., Elliot, G., Garrett, L., English, M.A., Andre, P., Robinson, J., Sood, R., Minami, Y., et al., 2011. Wnt Signaling gradients establish planar cell polarity by inducing Vangl2 phosphorylation through Ror2. Dev. Cell. 20, 163–176.

Garel, S., Garcia-Dominguez, M., Charnay, P., 2000. Control of the migratory pathway of facial branchiomotor neurones. Development 127, 5297–5307.

Goodrich, L.V., 2008. The plane facts of PCP in the CNS. Neuron 60, 9–16.

Grant, P.K., Moens, C.B., 2010. The neuroepithelial basement membrane serves as a boundary and a substrate for neuron migration in the zebrafish hindbrain. Neural Dev. 5, 9.

Habas, R., Kato, Y., He, X., 2001. Wnt/Frizzled activation of Rho regulates vertebrate gastrulation and requires a novel Formin homology protein Daam1. Cell 107, 843–854.

Hamblet, N.S., Lijam, N., Ruiz-Lozano, P., Wang, J., Yang, Y., Luo, Z., Mei, L., Chien, K.R., Sussman, D.J., Wynshaw-Boris, A., 2002. Dishevelled 2 is essential for cardiac outflow tract development, somite segmentation and neural tube closure. Development 129, 5827–5838.

Hatten, M.E., 2002. New directions in neuronal migration. Science 297, 1660–1663.

Higashijima, S., Hotta, Y., Okamoto, H., 2000. Visualization of cranial motor neurons in live transgenic zebrafish expressing green fluorescent protein under the control of the islet-1 promoter/enhancer. J. Neurosci. 20, 206–218.

Iliescu, A., Gravel, M., Horth, C., Kibar, Z., Gros, P., 2011. Loss of membrane targeting of Vangl proteins causes neural tube defects. Biochemistry 50, 795–804.

Jessen, J.R., Solnica-Krezel, L., 2004. Identification and developmental expression pattern of Van Gogh-like 1, a second zebrafish strabismus homologue. Gene Exprssion Patterns 4, 339–344.

Jessen, J.R., Topczewski, J., Bingham, S., Sepich, D.S., Marlow, F., Chandrasekhar, A., Solnica-Krezel, L., 2002. Zebrafish trilobite identifies new roles for Strabismus in gastrulation and neuronal movements. Nat. Cell Biol. 4, 610–615.

Kallay, L.M., McNickle, A., Brennwald, P.J., Hubbard, A.L., Braiterman, L.T., 2006. Scribble associates with two polarity proteins, Lgl2 and Vangl2, via distinct molecular domains. J. Cell Biochem. 99, 647–664.

Karis, A., Pata, I., van Doorninck, J.H., Grosveld, F., de Zeeuw, C.I., de Caprona, D., Fritzsch, B., 2001. Transcription factor GATA-3 alters pathway selection of olivocochlear neurons and affects morphogenesis of the ear. J. Comput. Neurol. 429, 615–630.

Kibar, Z., Underhill, D.A., Canonne-Hergaux, F., Gauthier, S., Justice, M.J., Gros, P., 2001. Identification of a new chemically induced allele (Lp(m1Jus)) at the loop-tail locus: morphology, histology, and genetic mapping. Genomics 72, 331–337.

Kraus, F., Haenig, B., Kispert, A., 2001. Cloning and expression analysis of the mouse T-box gene tbx20. Mech. Dev. 100, 87–91.

Lijam, N., Paylor, R., McDonald, M.P., Crawley, J.N., Deng, C.X., Herrup, K., Stevens, K.E., Maccaferri, G., McBain, C.J., Sussman, D.J., et al., 1997. Social interaction and sensorimotor gating abnormalities in mice lacking Dvl1. Cell 90, 895–905.

Lu, X., Borchers, A.G., Jolicoeur, C., Rayburn, H., Baker, J.C., Tessier-Lavigne, M., 2004. PTK7/CCK-4 is a novel regulator of planar cell polarity in vertebrates. Nature 430, 93–98.

Mapp, O.M., Walsh, G.S., Moens, C.B., Tada, M., Prince, V.E., 2011. Zebrafish Prickle1b mediates facial branchiomotor neuron migration via a farnesylation-dependent nuclear activity. Development 138, 2121–2132.

Mapp, O.M., Wanner, S.J., Rohrschneider, M.R., Prince, V.E., 2010. Prickle1b mediates interpretation of migratory cues during zebrafish facial branchiomotor neuron migration. Dev. Dyn. 239, 1596–1608.

Marin, O., Rubenstein, J.L., 2003. Cell migration in the forebrain. Annu. Rev. Neurosci. 26, 441–483.

Merte, J., Jensen, D., Wright, K., Sarsfield, S., Wang, Y., Schekman, R., Ginty, D.D., 2010. Sec24b selectively sorts Vangl2 to regulate planar cell polarity during neural tube closure. Nat. Cell. Biol. 12, 41–46, sup pp 1-8.

Montcouquiol, M., Rachel, R.A., Lanford, P.J., Copeland, N.G., Jenkins, N.A., Kelley, M.W., 2003. Identification of Vangl2 and Scrb1 as planar polarity genes in mammals. Nature 423, 173–177.

Montcouquiol, M., Sans, N., Huss, D., Kach, J., Dickman, J.D., Forge, A., Rachel, R.A., Copeland, N.G., Jenkins, N.A., Bogani, D., et al., 2006. Asymmetric localization of Vangl2 and Fz3 indicate novel mechanisms for planar cell polarity in mammals. J. Neurosci. 26, 5265–5275.

Mossie, K., Jallal, B., Alves, F., Sures, I., Plowman, G.D., Ullrich, A., 1995. Colon carcinoma kinase-4 defines a new subclass of the receptor tyrosine kinase family. Oncogene 11, 2179–2184.

Murdoch, J.N., Doudney, K., Paternotte, C., Copp, A.J., Stanier, P., 2001. Severe neural tube defects in the loop-tail mouse result from mutation of Lpp1, a novel gene involved in floor plate specification. Hum. Mol. Genet. 10, 2593–2601.

Nadarajah, B., Parnavelas, J.G., 2002. Modes of neuronal migration in the developing cerebral cortex. Nat. Rev. Neurosci. 3, 423–432.

Nagy, A., 2003. Manipulating the Mouse Embryo: A Laboratory Manual. Cold Spring Harbor Laboratory Press, Cold Spring Harbor, NY.

Nambiar, R.M., Ignatius, M.S., Henion, P.D., 2007. Zebrafish colgate/hdac1 functions in the non-canonical Wnt pathway during axial extension and in Wnt-independent branchiomotor neuron migration. Mech. Dev. 124, 682–698.

Ohsawa, R., Ohtsuka, T., Kageyama, R., 2005. Mash1 and Math3 are required for development of branchiomotor neurons and maintenance of neural progenitors. J. Neurosci. 25, 5857–5865.

Park, M., Moon, R.T., 2002. The planar cell-polarity gene stbm regulates cell behaviour and cell fate in vertebrate embryos. Nat. Cell Biol. 4, 20–25.

Pattyn, A., Hirsch, M., Goridis, C., Brunet, J.F., 2000. Control of hindbrain motor neuron differentiation by the homeobox gene Phox2b. Development 127, 1349–1358.

Paudyal, A., Damrau, C., Patterson, V.L., Ermakov, A., Formstone, C., Lalanne, Z., Wells, S., Lu, X., Norris, D.P., Dean, C.H., et al., 2010. The novel mouse mutant, chuzhoi, has disruption of Ptk7 protein and exhibits defects in neural tube, heart and lung development and abnormal planar cell polarity in the ear. BMC Dev. Biol. 10, 87.

Qu, Y., Glasco, D.M., Zhou, L., Sawant, A., Ravni, A., Fritzsch, B., Damrau, C., Murdoch, J.N., Evans, S., Pfaff, S.L., et al., 2010. Atypical cadherins Celsr1-3 differentially regulate migration of facial branchiomotor neurons in mice. J. Neurosci. 30, 9392–9401.

Ravni, A., Qu, Y., Goffinet, A.M., Tissir, F., 2009. Planar cell polarity cadherin celsr1 regulates skin hair patterning in the mouse. J. Invest. Dermatol. 129, 2507–2509.

Rohrschneider, M.R., Elsen, G.E., Prince, V.E., 2007. Zebrafish Hoxb1a regulates multiple downstream genes including prickle1b. Dev. Biol. 309, 358–372.

Shirasaki, R., Lewcock, J.W., Lettieri, K., Pfaff, S.L., 2006. FGF as a target-derived chemoattractant for developing motor axons genetically programmed by the LIM code. Neuron 50, 841–853.

Sittaramane, V., Sawant, A., Wolman, M.A., Maves, L., Halloran, M.C., Chandrasekhar, A., 2009. The cell adhesion molecule Tag1, transmembrane protein Stbm/Vangl2, and Lamininalpha1 exhibit genetic interactions during migration of facial branchiomotor neurons in zebrafish. Dev. Biol. 325, 363–373.

Sokol, S.Y., 1996. Analysis of Dishevelled signalling pathways during Xenopus development. Curr. Biol. 6, 1456–1467.

Song, H., Hu, J., Chen, W., Elliott, G., Andre, P., Gao, B., Yang, Y., 2010. Planar cell polarity breaks bilateral symmetry by controlling ciliary positioning. Nature 466, 378–382.

Song, M.R., 2007. Moving cell bodies: understanding the migratory mechanism of facial motor neurons. Arch. Pharm. Res. 30, 1273–1282.

Song, M.R., Shirasaki, R., Cai, C.L., Ruiz, E.C., Evans, S.M., Lee, S.K., Pfaff, S.L., 2006. T-Box transcription factor Tbx20 regulates a genetic program for cranial motor neuron cell body migration. Development 133, 4945–4955.

Tada, M., Concha, M.L., Heisenberg, C.P., 2002. Non-canonical Wnt signalling and regulation of gastrulation movements. Semin. Cell Dev. Biol. 13, 251–260.

Tada, M., Smith, J.C., 2000. Xwnt11 is a target of Xenopus Brachyury: regulation of gastrulation movements via Dishevelled, but not through the canonical Wnt pathway. Development 127, 2227–2238.

Thaler, J., Harrison, K., Sharma, K., Lettieri, K., Kehrl, J., Pfaff, S.L., 1999. Active suppression of interneuron programs within developing motor neurons revealed by analysis of homeodomain factor HB9. Neuron 23, 675–687.

Thoby-Brisson, M., Bouvier, J., Glasco, D.M., Stewart, M.E., Dean, C., Murdoch, J.N., Champagnat, J., Fortin, G., Chandrasekhar, A., 2012. Brainstem respiratory oscillators develop independently of neuronal migration defects in the Wnt/PCP mouse mutant looptail. PLoS One 7, e31140.

Tissir, F., Goffinet, A.M., 2006. Expression of planar cell polarity genes during development of the mouse CNS. Eur. J. Neurosci. 23, 597–607.

Tiveron, M.C., Pattyn, A., Hirsch, M.R., Brunet, J.F., 2003. Role of Phox2b and Mash1 in the generation of the vestibular efferent nucleus. Dev. Biol. 260, 46–57.

Torban, E., Kor, C., Gros, P., 2004a. Van Gogh-like2 (Strabismus) and its role in planar cell polarity and convergent extension in vertebrates. Trends Genet. 20, 570–577.

Torban, E., Wang, H.J., Groulx, N., Gros, P., 2004b. Independent mutations in mouse Vangl2 that cause neural tube defects in looptail mice impair interaction with members of the Dishevelled family. J. Biol. Chem. 279, 52703–52713.

Torban, E., Wang, H.J., Patenaude, A.M., Riccomagno, M., Daniels, E., Epstein, D., Gros, P., 2007. Tissue, cellular and sub-cellular localization of the Vangl2 protein during embryonic development: effect of the Lp mutation. Gene Expression Patterns 7, 346–354.

Vivancos, V., Chen, P., Spassky, N., Qian, D., Dabdoub, A., Kelley, M., Studer, M., Guthrie, S., 2009. Wnt activity guides facial branchiomotor neuron migration, and involves the PCP pathway and JNK and ROCK kinases. Neural Dev. 4, 7.

Wada, H., Iwasaki, M., Sato, T., Masai, I., Nishiwaki, Y., Tanaka, H., Sato, A., Nojima, Y., Okamoto, H., 2005. Dual roles of zygotic and maternal Scribble1 in neural migration and convergent extension movements in zebrafish embryos. Development 132, 2273–2285.

Wada, H., Tanaka, H., Nakayama, S., Iwasaki, M., Okamoto, H., 2006. Frizzled3a and Celsr2 function in the neuroepithelium to regulate migration of facial motor neurons in the developing zebrafish hindbrain. Development 133, 4749–4759.

Wallingford, J.B., Harland, R.M., 2002. Neural tube closure requires Dishevelled-dependent convergent extension of the midline. Development 129, 5815–5825.

Walsh, G.S., Grant, P.K., Morgan, J.A., Moens, C.B., 2011. Planar polarity pathway and Nance-Horan syndrome-like 1b have essential cell-autonomous functions in neuronal migration. Development 138, 3033–3042.

Wang, J., Hamblet, N.S., Mark, S., Dickinson, M.E., Brinkman, B.C., Segil, N., Fraser, S.E., Chen, P., Wallingford, J.B., Wynshaw-Boris, A., 2006. Dishevelled genes mediate a conserved mammalian PCP pathway to regulate convergent extension during neurulation. Development 133, 1767–1778.

Wang, J., Mark, S., Zhang, X., Qian, D., Yoo, S.J., Radde-Gallwitz, K., Zhang, Y., Lin, X., Collazo, A., Wynshaw-Boris, A., et al., 2005. Regulation of polarized extension and planar cell polarity in the cochlea by the vertebrate PCP pathway. Nat. Genet. 37, 980–985.

Westerfield, M., 1995. The Zebrafish Book: A Guide for the Laboratory Use of zebrafish (*Danio rerio*). M. Westerfield, Eugene, OR.

Ybot-Gonzalez, P., Savery, D., Gerrelli, D., Signore, M., Mitchell, C.E., Faux, C.H., Greene, N.D., Copp, A.J., 2007. Convergent extension, planar-cell-polarity signalling and initiation of mouse neural tube closure. Development 134, 789–799.